The Dynamics of the Reactions of Methyl Diphenylhydroperoxyacetate with [*meso*-Tetrakis(2,6-dimethyl-3-sulfonatophenyl)porphinato]-manganese(III) Hydrate and [*meso*-Tetrakis(2,6-dichloro-3-sulfonatophenyl)porphinato]-manganese(III) Hydrate and Imidazole Complexes. Comparison of the Reactions of Manganese(III) and Iron(III) Porphyrins†

Ramesh D. Arasasingham and Thomas C. Bruice*

Contribution from the Department of Chemistry, University of California at Santa Barbara, Santa Barbara, California 93106. *Received December 20, 1990*

Abstract: The reactions of $(Ph)_2(MeOCO)COOH$ with two water-soluble non-μ-oxo dimer-forming manganese(III) porphyrins, [*meso*-tetrakis(2,6-dimethyl-3-sulfonatophenyl)porphinato]manganese(III) hydrate, [(**1**)$Mn^{III}(X)_2$], and [*meso*-tetrakis(2,6-dichloro-3-sulfonatophenyl)porphinato]manganese(III) hydrate [(**2**)$Mn^{III}(X)_2$, where X = HO^- or H_2O], have been examined in aqueous solution [30 °C; μ = 0.2 (with $NaNO_3$); pH 5.3–12.6] and compared to the reaction with the iron porphyrin (**1**)$Fe^{III}(X)_2$. Kinetic studies were carried out in the presence and absence of imidazole, with the sodium salt of 2,2′-azinobis(3-ethylbenzthiazoline-6-sulfonic acid) (ABTS) as a trap for higher valent manganese porphyrin intermediates. Reactions were found to be first-order in both $[(porph)Mn^{III}(X)_2]_i$ and $[(Ph)_2(MeOCO)COOH]_i$ and independent of $[ABTS]_i$ and buffer concentrations {$H_2PO_4^-/HPO_4^{2-}$ (pH 7.3), HCO_3^-/CO_3^{2-} (pH 9.8), and 2,4,6-trimethylpyridine·H^+/2,4,6-trimethylpyridine (pH 8.4 and 7.5)}. Thus, the reactions are not subject to general base or general acid catalysis. A plot of the log of the pH-dependent second-order rate constant (k_{ly}) vs pH may be fit by an equation (eq 8) derived by assumption of steady state in the reactive species $(porph)Mn^{III}(OH)((Ph)_2(MeOCO)COOH)/(porph)Mn^{III}(H_2O)((Ph)_2(MeOCO)COO)$ and $[(porph)Mn^{III}(OH)((Ph)_2(MeOCO)COO)]^-$. Product analysis in the absence of ABTS provided 9% yield of $(Ph)_2CO$ and 81% yield of $(Ph)_2(MeOCO)COH$. In the presence of the ABTS trap $(Ph)_2CO$ is formed in 12% yield, and the main product is again $(Ph)_2(MeOCO)COH$ (55%). In reactions with (**1**)$Mn^{III}(X)_2$ and (**2**)$Mn^{III}(X)_2$ (pH 5.3–12.6) a high spin, d^3, manganese(IV) intermediate (μ = 3.90 μ_B at 295 K) was observed. A comparison of the log k_{ly} vs pH profiles for the reaction of (**1**)$Mn^{III}(X)_2$ and (**1**)$Fe^{III}(X)_2$ with $(Ph)_2(MeOCO)COOH$ showed that k_{ly} values are comparable at high pH while at lower pH, (**1**)$Fe^{III}(X)_2$ is far more reactive. This difference in log k_{ly} vs pH profiles for (**1**)$Mn^{III}(X)_2$ vs (**1**)$Fe^{III}(X)_2$ finds explanation in the differing pH dependence of potentials for $1e^-$ reduction of Mn(IV) and Fe(IV) species. Addition of imidazole resulted in an enhancement in the rate of reaction. Apparent equilibrium constants were determined at various values of pH for monoligation of imidazole, and the dependence of rate on pH was employed to show that the reactive intermediates are (i) low pH, $[(1)Mn^{III}(ImH)((Ph)_2(MeOCO)COOH)]^+$; (ii) intermediate pH, $(1)Mn^{III}(Im)((Ph)_2(MeOCO)COOH)/(1)Mn^{III}(ImH)((Ph)_2(MeOCO)COO)$; and (iii) high pH, $[(1)Mn^{III}(Im)((Ph)_2(MeOCO)COO)]^-$. Imidazole ligation provided at most a rate enhancement of ~100-fold.

Introduction

The mechanisms of reactions of metalloporphyrins with organic hydroperoxides have received considerable attention because of their relevance to the mechanisms of several classes of iron(III) protoporphyrin IX containing enzymes that include peroxidases,[1] catalases,[2] and the "peroxide shunt" mechanism of cytochrome P-450 enzymes.[3] Intensive studies on the hydroperoxide oxidations of iron(III) porphyrin complexes have suggested that the metal center reacts with hydroperoxides by a mechanism that is different from that observed for peracids. It is generally agreed that peracids transfer an oxygen atom with concomitant two-electron oxidation of iron(III) porphyrin (the result of heterolytic cleavage of the O–O bond, eq 1) to form an iron(IV)–oxo porphyrin π-cation radical, which is capable of epoxidizing alkenes.[4,5] A

$$[(porph)Fe^{III}]^+ + RCO_3H \rightarrow [(^{+\bullet}porph)Fe^{IV}{=}O] + RCO_2H \quad (1)$$

similar apoenzyme bound iron(IV)–oxo protoporphyrin IX π-cation radical has been established as the reactive compound I intermediate of horseradish peroxidase and catalase formed upon reaction with hydroperoxides.[1,2] In nonenzymatic studies, however, considerable evidence has been offered in support of the one-electron oxidation of *meso*-tetraphenylporphyrin iron(III) species by hydroperoxides to provide iron(IV)–oxo porphyrin species (eq 2).[6-8d-g] The reaction of eq 2 represents a homolysis of the O–O

† Abbreviations used: **1**, *meso*-tetrakis(2,6-dimethyl-3-sulfonatophenyl)-porphyrin dianion; **2**, *meso*-tetrakis(2,6-dichloro-3-sulfonatophenyl)porphyrin dianion; porph, generic porphyrin dianion; X, H_2O or HO^-; ImH, imidazole; ROOH, $(Ph)_2(MeOCO)COOH$.

(1) (a) Saunders, B. C.; Holmes-Siedel, A. G.; Stark, B. P. *Peroxidases*; Butterworths: London, 1964. (b) Hewson, W. D.; Hager, L. D. *Porphyrins* **1979**, *7*, 295. (c) Saunders, B. C. In *Inorganic Biochemistry*; Eichorn, G. I., Ed.; Elsevier: Amsterdam, The Netherlands, 1973; Vol. 2, p 988. (d) Dunford, H. B. *Ad. Inorg. Biochem.* **1982**, *4*, 41. (e) Dunford, H. B.; Stillman, J. S. *Coord. Chem. Rev.* **1976**, *19*, 187.

(2) Schonbaum, G. R.; Chance, B. Catalase In *The Enzymes*; Boyer, P., Ed.; Academic Press: New York, 1976; Vol. 13, p 363.

(3) Ortiz de Montellano, P. *Cytochrome P450: Structure, Mechanism and Biochemistry*: Plenum Press: New York, 1986.

(4) (a) Lee, W. A.; Bruice, T. C. *J. Am. Chem. Soc.* **1985**, *107*, 513. (b) Lee, W. A.; Yuan, L.-C.; Bruice, T. C. *J. Am. Chem. Soc.* **1988**, *110*, 4277.

(5) (a) Groves, J. T.; Haushaulter, R. C.; Nakamura, M.; Nemo, T. E.; Evans, B. J. *J. Am. Chem. Soc.* **1981**, *103*, 2884. (b) Groves, J. T.; Watanabe, Y. *J. Am. Chem. Soc.* **1986**, *108*, 7834. (c) Penner-Hahn, J. E.; Elbe, K. S.; McMurry, T. J.; Renner, M. R.; Balch, A. L.; Groves, J. T.; Dawson, J. H.; Hodgson, K. O. *J. Am. Chem. Soc.* **1986**, *108*, 7819.

(6) Labeque, R.; Marnett, L. *J. Am. Chem. Soc.* **1989**, *111*, 6621.

(7) (a) Arasasingham, R. D.; Cornman, C. R.; Balch, A. L. *J. Am. Chem. Soc.* **1989**, *111*, 7800. (b) Balch, A. L.; Hart, R. L.; Latos-Grazynski, L.; Traylor, T. G. *J. Am. Chem. Soc.* **1990**, *112*, 7382.

0002-7863/91/1513-6095$02.50/0

hydroperoxide bond. Unlike the iron(IV)–oxo porphyrin π-cation

$$[(\text{porph})\text{Fe}^{\text{III}}]^+ + \text{ROOH} \rightarrow [(\text{porph})\text{Fe}^{\text{IV}}{=}\text{O}] + \text{RO}^\bullet + \text{H}^+ \quad (2)$$

radical species, the iron(IV)–oxo porphyrin species is, at best, a very ineffective epoxidizing species. Other kinetic and product studies on the epoxidation of alkenes by hydroperoxides and iron(III) tetraphenylporphyrins have been offered in support of a heterolytic mechanism. These evidences[9] are considered controversial and are discussed elsewhere.[10] Additionally, in the presence of imidazole, iron(III), and manganese(III) tetraphenylporphyrins have been found to be better catalysts for epoxidation with hydroperoxides. And, in the case of manganese porphyrins, evidence has been presented for the formation of a transient species described as a high-valent manganese–oxo species.[11]

The mechanism(s) of reactions of metal(III) porphyrins with hydroperoxides constitutes an ongoing study in our laboratory. Recognizing the limitations of studies on the dynamics of reactions involving dissociable protons in organic media, we have included studies in aqueous solutions where a precise knowledge of the proton activity and acid dissociation constants of starting materials and intermediates can be known.[8] Previous studies in aqueous medium have dealt with the mechanisms of reactions of several alkyl hydroperoxides (*t*-BuOOH, $Ph(Me)_2COOH$, and $(Ph)_2(MeOCO)COOH$) with the water-soluble non-μ-oxo dimer-forming [*meso*-tetrakis(2,6-dimethyl-3-sulfonatophenyl)porphinato]iron(III) hydrate, $[(\mathbf{1})\text{Fe}^{\text{III}}(X)_2]$, and [*meso*-tetrakis(2,6-dichloro-3-sulfonatophenyl)porphinato]iron(III) hydrate $[(\mathbf{2})\text{Fe}^{\text{III}}(X)_2$, where X = HO^- or H_2O]. From these studies, it has been established that the structure of the hydroperoxide-coordinated iron(III) porphyrin complexes are pH dependent as is the rate of decomposition.

In the present investigation we explore the effect of change in the porphyrin ligated metal from Fe(III) to Mn(III). In order to determine the second-order rate constants over as broad a range of pH as possible we have chosen the reactive hydroperoxide $(Ph)_2(MeOCO)COOH$ as substrate. This choice was made on the basis of a previous investigation in organic solvents[12] on the reaction of [*meso*-tetraphenylporphinato]manganese(III) chloride with acyl and alkyl hydroperoxides (eq 3). An inordinant sensitivity of the rate constant to the pK_a of the leaving group ($\beta_{lg} = -1.25$) was shown. Indeed, the reaction with *t*-BuOOH could not be measured.

$$(\text{porph})\text{Mn}^{\text{III}}(\text{Cl}) + \text{ROOH} \rightarrow (\text{porph})\text{Mn}^{\text{V}}(\text{O})(\text{Cl}) + \text{ROH} \quad (3)$$

We report here the results of a study on the reaction of $(Ph)_2(MeOCO)COOH$ with two manganese(III) porphyrins, $(\mathbf{1})\text{Mn}^{\text{III}}(X)_2$ and $(\mathbf{2})\text{Mn}^{\text{III}}(X)_2$, in the presence and absence of imidazole.

Experimental Section

Materials. Deionized, double-glass distilled water was used for all experiments. The disodium salt of 2,2′-azinobis(3-ethylbenzthiazoline)sulfonic acid (ABTS) was prepared[8i] from the diammonium salt (Sigma Chemical Co.). The hydroperoxide, $(Ph)_2(MeOCO)COOH$, was prepared as described previously,[8g] and its purity was determined by iodometric analysis[13] prior to use. Imidazole was twice recrystallized from benzene. 2,4,6-Trimethylpyridine was purified by conversion to its HCl salt by a previously described procedure.[8i] All the buffer and salt solutions were prepared from reagent-grade chemicals and passed through a Chelex 100 column or extracted with 0.01% dithiazone in dichloromethane to remove possible heavy metal contaminants.

$(\mathbf{1})H_2$ and $(\mathbf{2})H_2$ were prepared by a previously reported procedure,[8] and the insertion of manganese was accomplished by the method described by Balasubramanian et al.[8c] Anal. Calcd for $(C_{44}H_{16}Cl_8N_4S_4O_{12}Na_4)\text{Mn(OH)}\cdot 20H_2O \times 0.5\ Na_2SO_4 \times 2.5\ SO_4^{2-}$ (fw 2034.67): C, 2.82; H, 25.95; N, 2.75; Na, 5.65; S, 11.0; Cl, 13.75; Mn, 2.70. Found: C, 2.65; H, 25.42; N, 3.58; Na, 5.74; S, 11.09; Cl, 13.09; Mn, 2.40.

Instrumentation. Kinetic studies and absorption measurements were conducted with either a Perkin-Elmer 553 spectrophotometer or a Cary 14 spectrophotometer interfaced to a Zenith computer equipped with OLIS (On-Line Instrument System Inc.). The cell compartments were thermostated at 30 °C. A Hewlett-Packard 9825A computer, equipped with a 9864A digitizer and plotter, was employed for the analysis of the kinetic traces and pH-rate profiles, with the appropriate software programs written for these purposes. pH measurements were carried out with a Radiometer Model pH M26 with metrohm electrode, and NMR measurements were recorded on a Nicolet NT 300 Fourier-transform spectrophotometer. HPLC was performed with a Perkin-Elmer Series 10 pump connected to an Whatman Partisil 5 ODS-3 column (250 mm). Product quantitation was performed with a Hewlett-Packard variable wavelength detector (Model HP1050) at 235 nm interfaced to a Hewlett-Packard HP3392A integrator.

Results

The water-soluble manganese(III) porphyrins, $(\mathbf{1})\text{Mn}^{\text{III}}(\text{OH})(H_2O)$ and $(\mathbf{2})\text{Mn}^{\text{III}}(\text{OH})(H_2O)$, displayed three spots (of identical visible spectra) when subjected to reversed-phase thin-layer chromatography.[8c] This observation indicates that the $(\mathbf{1})\text{Mn}^{\text{III}}(\text{OH})(H_2O)$ and $(\mathbf{2})\text{Mn}^{\text{III}}(\text{OH})(H_2O)$ samples comprised of at least three of the four possible atropisomers. However, determination of the pK_a of $(\mathbf{1})\text{Mn}^{\text{III}}(\text{OH})(H_2O)$ has clearly demonstrated that all the atropisomers possess indistinguishable pK_a values, indicating the electronic nature of the manganese(III) center in all the isomers to be the same.[8c] Consequently, their kinetic behavior should also be indistinguishable.

Kinetics of the reaction of $(\mathbf{1})\text{Mn}^{\text{III}}(X)_2$ and $(\mathbf{2})\text{Mn}^{\text{III}}(X)_2$ with $(Ph)_2(MeOCO)COOH$ (ROOH), in aqueous medium, was examined between pH 5.3 and 12.6 (30 °C; $\mu = 0.2$ with $NaNO_3$) by the use of the sodium salt of 2,2′-azinobis(3-ethylbenzthiazoline-6-sulfonic acid) (ABTS) as an easily oxidizable trap for the reactive higher valent manganese porphyrin intermediates and any radical products derived from $(Ph)_2(MeOCO)COOH$. The one-electron oxidation of ABTS to provide the bluish green radical $ABTS^{\bullet+}$ was followed spectrophotometrically at 660 nm as described previously.[8b] Reactions were carried out under the conditions of $[(\text{porph})\text{Mn}^{\text{III}}(X)_2] < [\text{ROOH}] \ll [\text{ABTS}]$.

The Dependence of k_{obsd} (s^{-1}) on the Concentrations of Trapping Agent and Reactants. The values for k_{obsd} were determined over a 10-fold change in concentration of $(\mathbf{1})\text{Mn}^{\text{III}}(X)_2$ (5.3×10^{-6}–5.3×10^{-5} M) while maintaining the initial concentrations of $[\text{ROOH}]_i$ and $[\text{ABTS}]_i$ (1.0×10^{-2} M) constant. Reactions were initiated by addition of a freshly prepared methanolic solution of ROOH to a final concentration of 1.6×10^{-5} M [H_2O/MeOH (v/v) 100/1]. At pH values below 5, the reaction of $(\text{porph})\text{Mn}^{\text{III}}(X)_2$ with ROOH was quite slow such that the rate of "spontaneous" decomposition of ROOH exceeds the rate of its reaction with the manganese(III) porphyrins. Thus, in this pH range the rate of reaction is independent of the presence of $(\text{porph})\text{Mn}^{\text{III}}(X)_2$. Between pH 5 and 7, the method of initial

(8) (a) Bruice, T. C.; Zipplies, M. F.; Lee, W. A. *Proc. Natl. Acad. Sci. U.S.A.* **1986**, *83*, 4646. (b) Zipplies, M. F.; Lee, W. A.; Bruice, T. C. *J. Am. Chem. Soc.* **1986**, *108*, 4433. (c) Balasubramanian, P. N.; Schmidt, E. S.; Bruice, T. C. *J. Am. Chem. Soc.* **1987**, *109*, 7865. (d) Lindsay Smith, J. R.; Balasubramanian, P. N.; Bruice, T. C. *J. Am. Chem. Soc.* **1988**, *110*, 7411. (e) Bruice, T. C.; Balasubramanian, P. N.; Lee, R. W.; Lindsay Smith, J. R. *J. Am. Chem. Soc.* **1988**, *110*, 7890. (f) Balasubramanian, P. N.; Lindsay Smith, J. R.; Davies, M. J.; Kaaret, T. W.; Bruice, T. C. *J. Am. Chem. Soc.* **1989**, *111*, 1477. (g) Balasubramanian, P. N.; Lee, R. W.; Bruice, T. C. *J. Am. Chem. Soc.* **1989**, *111*, 8714. (h) Garrison, J. M.; Lee, R. W.; Bruice, T. C. *Inorg. Chem.* **1990**, *29*, 2019. (i) Panicucci, R.; Bruice, T. C. *J. Am. Chem. Soc.* **1990**, *112*, 6063. (j) Murata, K.; Panicucci, R.; Gopinath, E.; Bruice, T. C. *J. Am. Chem. Soc.* **1990**, *112*, 6072. (k) Gopinath, E.; Bruice, T. C. *J. Am. Chem. Soc.* **1991**, *113*, 4657. (l) Gopinath, E.; Bruice, T. C. Preceding paper in this issue.

(9) (a) Traylor, T. G.; Fann, W. D.; Bandyopadhyay, D. J. *J. Am. Chem. Soc.* **1989**, *111*, 8009. (b) Traylor, T. G.; Ciccone, J. P. *J. Am. Chem. Soc.* **1989**, *111*, 8413.

(10) He, G.-X; Bruice, T. C. *J. Am. Chem. Soc.* **1991**, *113*, 2747.

(11) (a) Mansuy, D.; Bartoli, J.-F.; Momenteau, M. *Tetrahedron Lett.* **1982**, *23*, 2781. (b) Mansuy, D.; Battioni, P.; Renaud, J.-P. *J. Chem. Soc., Chem. Commun.* **1984**, 1255.

(12) Yuan, L. C.; Buice, T. C. *Inorg. Chem.* **1985**, *24*, 986.

(13) Bruice, T. C.; Noar, J. B.; Ball, S. S.; Venkataram, U. V. *J. Am. Chem. Soc.* **1983**, *105*, 2452.

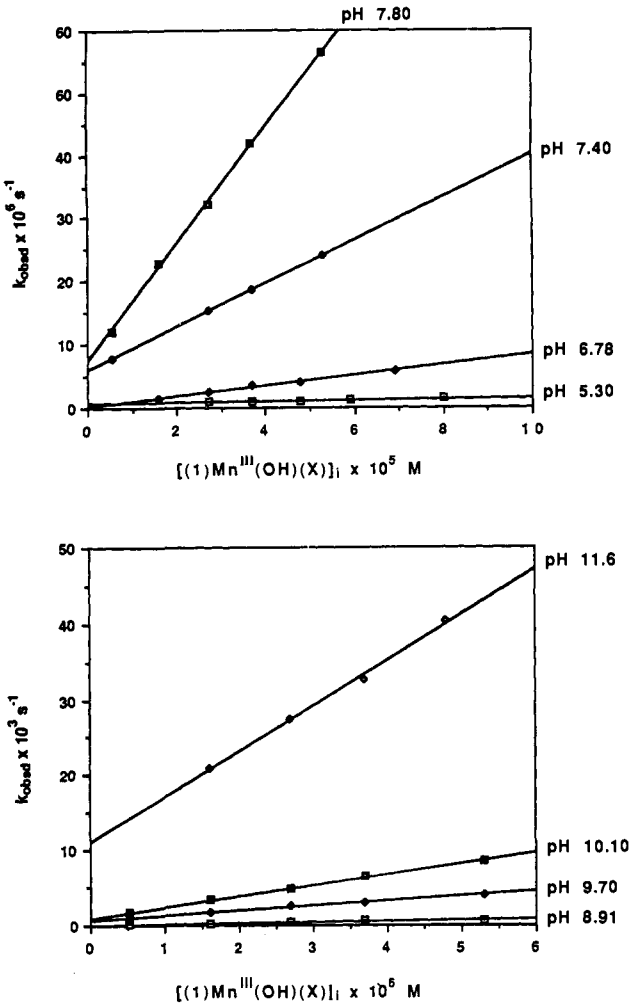

Figure 1. Plots of the pseudo-first-order rate constants (k_{obsd}) at pH 5.30, 6.78, 7.40, 7.80, and 8.91 (30 °C, μ = 0.2) for the formation of $ABTS^{\bullet+}$ as a function of $[(1)Mn^{III}(X)_2]$. The initial concentrations of $(Ph)_2(MeOCO)COOH$ and ABTS were 6.5×10^{-5} and 1.0×10^{-2} M, respectively.

rates was employed for the slower reactions (eq 4, where k_i = initial rate; A = absorbance at 660 nm; k_2 = apparent second-order rate

$$k_i = \frac{\Delta A_{ABTS^{\bullet+}}}{\Delta t} = k_2[ROOH][(porph)Mn^{III}(X)_2]2\epsilon_{ABTS^{\bullet+}} \quad (4)$$

constant; and $\epsilon_{ABTS^{\bullet+}}$ = molar extinction coefficient of $ABTS^{\bullet+}$). At pH 7–9 the appearance of $ABTS^{\bullet+}$ (ΔA_{660}) was found to follow the first-order rate law (k_{obsd}), while at pH values of >9 $ATBS^{\bullet+}$ formation was succeeded by its disappearance. The latter observation is explained by eq 5[8k] such that the value of k_1 (k_{obsd})

$$ABTS \xrightarrow{k_1} ABTS^{\bullet+} \xrightarrow{k_2} ABTS^{2+} \quad (5)$$

was obtained by fitting ΔA_{660} with time to the appropriate equation for sequential first-order reactions. Throughout the pH range investigated, k_{obsd} increased linearly as a function of $[(1)Mn^{III}(X)_2]$ at any given pH value. Figure 1 shows a sampling of the data obtained at pH 5.30, 6.78, 7.40, 7.80, 8.91, 9.70, 10.10, and 11.60. Thus, the reaction with ROOH is first-order in $(1)Mn^{III}(X)_2$.

The order of the reaction with ABTS was determined at constant $[(1)Mn^{III}(X)_2]_i$ (5.3×10^{-6} M) and $[ROOH]_i$ (6.5×10^{-5} M) at pH 7.78 ($H_2PO_4^-/HPO_4^{2-}$ buffer), while $[ABTS]_i$ was varied 10-fold (1.0×10^{-3}–1.0×10^{-2} M). The resulting k_{obsd} values (1.2×10^{-5}–1.3×10^{-5} s^{-1}) were constant indicating the appearance of $ABTS^{\bullet+}$ to be zero-order in ABTS.

The above experiments establish that the reaction of interest is first-order in both $[(1)Mn^{III}(X)_2]$ and [ROOH] and zero-order in [ABTS]. The oxidation of $(porph)Mn^{III}(X)_2$ by ROOH to form the intermediate higher valent porphyrin is rate-limiting so that $ABTS^{\bullet+}$ formation follows eq 6.

$$d[ABTS^{\bullet+}]/dt = k_{ly}[(porph)Mn^{III}(X)_2][ROOH] \quad (6)$$

where

$$k_{obsd} = k_{ly}[(porph)Mn^{III}(X)_2] \quad (7)$$

Table I. Values of the Second-Order Rate Constants for the reaction of (1) $Mn^{III}(X)_2$ and (2) $Mn^{III}(X)_2$ with $(Ph)_2(MeOCO)COOH$ at Various $[B_T]$ and pH Values (30 °C and μ = 0.2 with $NaNO_3$)

pH	buffer	$[B_T]$, mM	k_{ly}; $M^{-1}\ s^{-1}$
		$(1)Mn^{III}(X)_2$	
7.34	phosphate	50.0	0.35
		5.0	0.35
9.79	carbonate	50.0	101
		5.0	115
8.44	2,4,6-trimethylpyridine	53.0	6.38
		37.1	6.63
		21.7	6.63
		5.3	5.79
7.47	2,4,6-trimethylpyridine	50.0	0.84
		5.0	0.66
		$(2)Mn^{III}(X)_2$	
7.28	phosphate	50.0	0.74
		5.0	0.70
9.79	carbonate	50.0	75.8
		5.0	76.6

Table II. Values of Apparent Rate and Equilibrium Constants Obtained from the Fitting of Eq 8 to the Experimental Points in Figure 2 (30 °C and μ = 0.2 with $NaNO_3$)

equiv kinetic terms (units in mol s)	Values of determined constants	
	$(1)Mn^{III}(X)_2$	$(2)Mn^{III}(X_2)$
k_a	3.86×10^{-3}	7.01×10^{-2}
K_{app}	1.34×10^{-8}	1.77×10^{-8}
k_b	7.69×10^{-4}	2.02×10^{-3}

Effect of Buffers on the Rate of Reaction of $(1)Mn^{III}(X)_2$ and $(2)Mn^{III}(X)_2$ with ROOH. The effects of buffers on k_{ly} were obtained by determining the k_{obsd} at constant values of pH and constant initial concentrations of $(1)Mn^{III}(X)_2$ or $(2)Mn^{III}(X)_2$ and ROOH while varying the total buffer concentration ($[B_T] = [B:] + [BH^+]$ = 5–50 mM). The following buffers were used: $H_2PO_4^-/HPO_4^{2-}$ (pH 7.3), HCO_3^-/CO_3^{2-} (pH 9.8), and 2,4,6-trimethylpyridine·H^+/2,4,6-trimethylpyridine (pH 8.4 and 7.5). As shown in Table I, the second-order rate constant k_{ly} is insensitive to a 10-fold change in $[B_T]$ for the various buffers used including the nitrogen buffer 2,4,6-trimethylpyridine.

Dependence of k_{ly} on pH for the Reaction of $(1)Mn^{III}(X)_2$ and $(2)Mn^{III}(X)_2$ with ROOH and the pH Dependence of the "Spontaneous" Decomposition of ROOH. The values of the second-order rate constants k_{ly} (eq 6) were determined in the pH range 5.3–12.6. Buffers employed were $H_2PO_4^-/HPO_4^{2-}$ (pH 5.3–7.8), HCO_3^-/CO_3^{2-} (pH 8.8–10.1), and H_2O/HO^- (pH 10.1 and above). The fitting of the kinetic data was carried out with five to six concentrations of $(porph)Mn^{III}(X)_2$ at each pH value, and in each case the rate constants (k_{obsd}) were found to be linearly dependent on $(porph)Mn^{III}(X)_2$. The second-order rate constants (k_{ly}) were obtained from the slopes of the linear plots of k_{obsd} vs $[(porph)Mn^{III}(X)_2]$. At most pH values, the plots were found to have nonzero intercepts indicating some slow decomposition of ROOH by a process independent of $[(porph)Mn^{III}(X)_2]$. A plot of the dependence upon pH of the intercepts of plots of k_{obsd} vs $[(porph)Mn^{III}(X)_2]$ (Figure 2) indicates that the lyate species catalysis of ROOH decomposition is first order in $[HO^-]$.

The pH dependence of the buffer-independent second-order rate constants (k_{ly}) for the reaction of ROOH with $(1)Mn^{III}(X)_2$ and $(2)Mn^{III}(X)_2$ are shown in Figure 3, where the experimental points were fit to the empirical eq 8 (standard error for $(1)Mn^{III}(X)_2$ = 3.61×10^{-2} and for $(2)Mn^{III}(X)_2$ = 4.59×10^{-2}). The values

$$k_{ly} = [k_a a_H/(K_{app} + a_H)] + [k_b K_{app}/(K_{app} + a_H)] \quad (8)$$

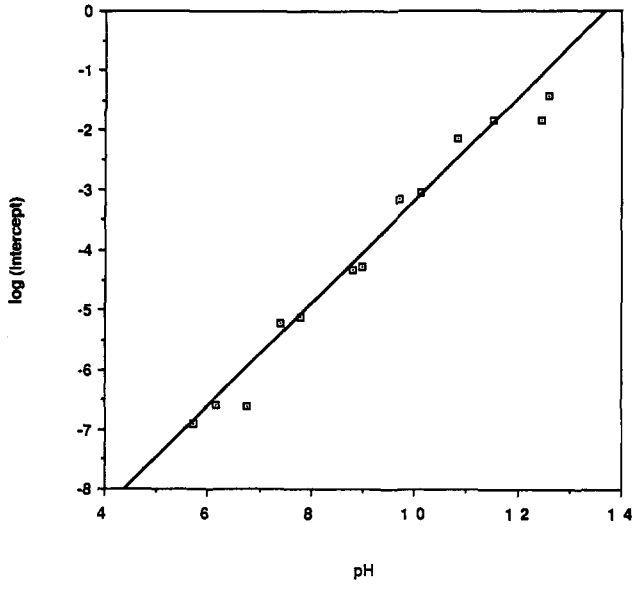

Figure 2. The pH dependence of the intercepts of plots of k_{obsd} vs $[(1)Mn^{III}(X)_2]_i$.

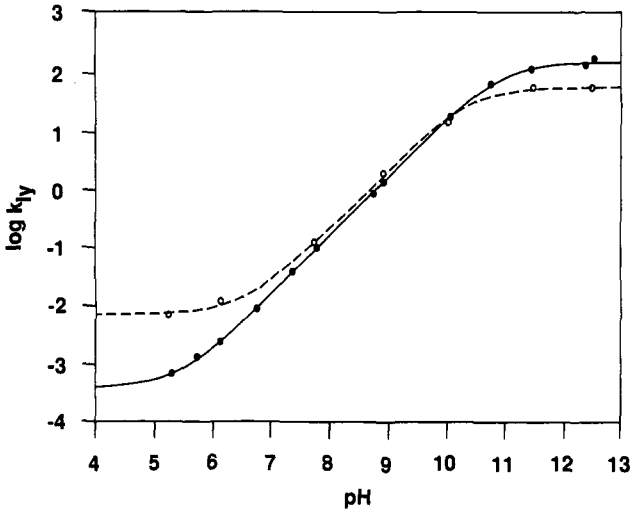

Figure 3. The pH dependence of the log of the nonbuffer-catalyzed second-order rate constants (k_{ly}) for the reaction of $(1)Mn^{III}(X)_2$ (—) and $(2)Mn^{III}(X)_2$ (--) with $(Ph)_2(MeOCO)COOH$. The points are experimentally determined rate constants for $ABTS^{\bullet+}$ formation (30 °C, μ = 0.2), and the curve are generated from eq 8.

for the derived constants are given in Table II.

Product analysis (pH 8.98, μ = 0.2) on the reaction of $(Ph)_2(MeOCO)COOH$ (1.08×10^{-3} M) with $(1)Mn^{III}(X)_2$ (6.4×10^{-5} M) by HPLC (reverse phase, with MeOH/H_2O (70/30, v/v) as the mobile phase) with freshly spent reaction solutions provided only benzophenone and $(Ph)_2(MeOCO)COH$. The reactions were examined in the presence and absence of ABTS. Without the ABTS, yields of benzophenone (9%) and $(Ph)_2(MeOCO)COH$ (81%) accounted for 90% of the total hydroperoxide employed. In the presence of ABTS (1.1×10^{-2} M) the yields were $(Ph)_2(MeOCO)COH$ (55%) and benzophenone (12%). Hydroxide attack upon $(Ph)_2(MeOCO)COOH$ becomes important at pH 12.60 (Figure 2), and the product of the reaction has been shown to be benzophenone.[81] Reactions at this pH in the presence of $(1)Mn^{III}(X)_2$ (6.4×10^{-5} M) with $[(Ph)_2(MeOCO)COOH]_i$ (9.8×10^{-4} M) provided benzophenone as the only observable product in the presence of ABTS (1.0×10^{-2} M) and in its absence. Complications in the interpretation of product yields with $(Ph)_2(MeOCO)COOH$ are discussed in the preceding paper in this issue.[81] Because of the instability of the alcohol and the reactivity of the hydroperoxide, the reported product yields are of little use in any consideration of mechanism.

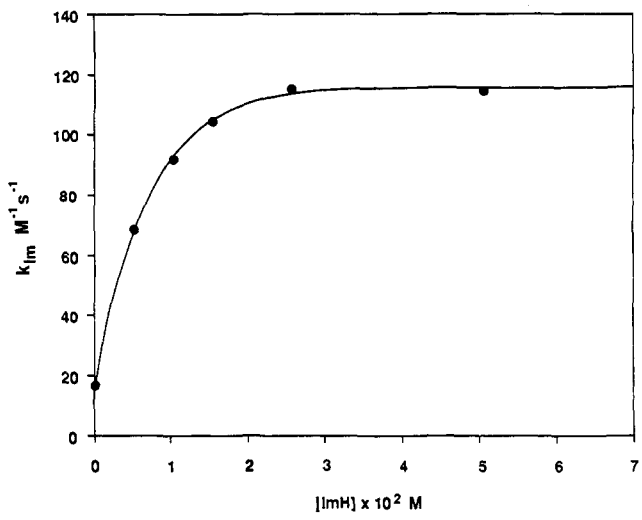

Figure 4. Plot of the apparent second-order rate constant (k_{Im}) vs [ImH]. $[(1)Mn^{III}(X)_2]_i = 5.12 \times 10^{-6}$ M, $[(Ph)_2(MeOCO)COOH]_i = 6.46 \times 10^{-5}$ M, $[ABTS]_i = 1.0 \times 10^{-2}$ M, pH 8.76 (50 mM phosphate buffer, μ = 0.2 with $NaNO_3$) at 30 °C.

Dependence of the reaction rate on the concentration of imidazole (ImH) for the reaction of $(1)Mn^{III}(X)_2$ with ROOH was determined in the pH range of 5.3–12.6 at constant $[(1)Mn^{III}(X)_2]_i$, $[ROOH]_i$ and $[ABTS]_i$. A typical reaction mixture contained a buffered solution of 1.0×10^{-2} M ABTS, 5.1×10^{-6} M $(1)Mn^{III}(X)_2$, and ImH in concentrations ranging from 0 to 5.0×10^{-2} M. Reactions were initiated by addition of a freshly prepared methanolic solution of ROOH to a final concentration of 6.5×10^{-5} M. A representative plot of the second-order rate constants (k_{Im}) determined at pH 8.76 vs $[imidazole]_i$ is shown in Figure 4. As found in a previous study[8c] of the reaction of $(1)Mn^{III}(X)_2$ with H_2O_2, such plots have nonzero intercepts, and the rate constants reach limiting values with increase in imidazole concentration. However, at pH values above ~12, the rate constants do not reach limiting values due to competition with $[HO^-]$. The dependence of k_{Im} (eq 9) on $[ImH]_i$ can be analyzed by use of eq 10, where k_{ly} is defined as before, K_1 is the the equilibrium

$$d[ABTS^{\bullet+}]/dt = -d[ROOH]/dt = k_{Im}[(1)Mn^{III}(X)_2][ROOH] \quad (9)$$

$$k_{obsd} = k_{Im}[(1)Mn^{III}(X)_2]$$

$$\text{where} \quad k_{Im} = \frac{k_{ly} + K_1 k_b[ImH]}{1 + K_1[ImH]} \quad (10)$$

constant for ImH monoligation, and k_b the rate constant for the reaction of imidazole-ligated manganese(III) porphyrin. It has previously been established, from spectrophotometric titrations, that $(1)Mn^{III}(X)_2$ ligates to only one ImH.[8c] The equilibrium constant K_1 for the monoligation may be calculated from the ratio (slope/intercept) of plots of $(1/k_{Im})[ImH]$ vs [ImH] (Figure 5) obtained by rearrangment of eq 10 to eq 11. Determined log K_1 (M^{-1}) values (at μ = 0.2) are as follows: 2.29, pH 5.28; 2.25, pH 6.78; 2.06, pH 7.75; 2.49, pH 8.76; 2.62, pH 9.30; 2.75, pH 9.60; 2.63, pH 10.01; 2.88, pH 10.49; 2.01, pH 11.43; and 2.28, pH 12.50. Thus, the equilibrium constant for monoligation of ImH to $(1)Mn^{III}(X)_2$ is pH independent (average value of log K_1 being 2.43 ± 0.05 M^{-1}).

$$(1/k_{Im})[ImH] = \frac{1}{k_{ly}[ImH]^{-1} + K_1 k_b} + \frac{K_1[ImH]}{k_{ly}[ImH]^{-1} + K_1 kb} \quad (11)$$

The log k_{Im} vs pH profile for the reaction of ROOH with $(1)Mn^{III}(ImH)(X)$ is shown in Figure 6. By definition, at saturation in ImH the values of $k_b = k_{Im}$, at any given pH. The experimental points were fit to the empirical eqs 12 (Figure 6—inset, standard error = 6.30×10^{-2}) and 13 (Figure 6, standard

$$k_{Im} = K_c + [k_d K_D/(K_D + a_H)] + [k_e K_E/(K_E + a_H)] \quad (12)$$

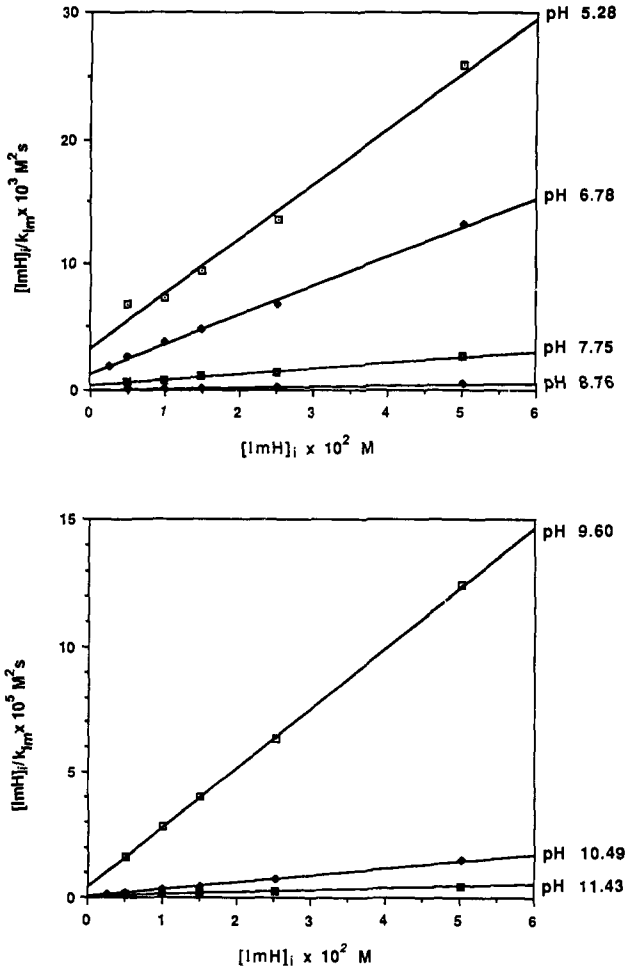

Figure 5. Plots of $(1/k_{Im})[ImH]$ vs [ImH] at different pH values.

Table III. Values of Rate and Equilibrium Constants Obtained from the Fitting of Eq 13 to the Experimental Points in Figure 7 (30 °C and μ = 0.2 with $NaNO_3$)

equiv kinetic terms (units in mol s)	values of determined constants
k_f	1.55
K_F	4.73×10^{-9}
k_g	60.8
k_h	1.92×10^{4}
K_H	4.96×10^{-12}

error = 5.86×10^{-2}). The better fit is to eq 13 (see Discussion). The values for the derived constants with eq 13 are given in Table III.

$$k_{Im} = [k_f a_H/(K_F + a_H)] + [k_g K_F a_H/(a_H^2 + K_F a_H + K_F K_H)] + [k_h K_H/(K_H + a_H)] \quad (13)$$

The formation of an observable higher valent manganese species upon reaction of (1)$Mn^{III}(X)_2$ or (2)$Mn^{III}(X)_2$ (5.3×10^{-6} M) with ROOH (6.6×10^{-5} M) was examined spectrophotometrically by repetitive scanning between 350 and 800 nm. At pH 8.9, the absorbance of the Soret peak of the manganese(III) porphyrin (465 nm for (1)$Mn^{III}(X)_2$ and 468 nm for (2)$Mn^{III}(X)_2$) decreased in concert with the formation of a higher valent manganese species (423 nm for (1)$Mn^{III}(X)_2$ and 424 nm for (2)$Mn^{III}(X)_2$). The samples showed mixtures of the manganese(III) porphyrin and the higher valent species throughout the course of the reaction. However, at pH 12.6, the formation of the higher valent species is complete upon addition of ROOH (Figure 7). After all the ROOH was consumed the higher valent manganese species was stable for several hours and slowly decomposed over a ~24-h period to regenerate the original manganese(III) porphyrin. Addition of ABTS (1.0×10^{-3} M) to the solution rapidly reduced

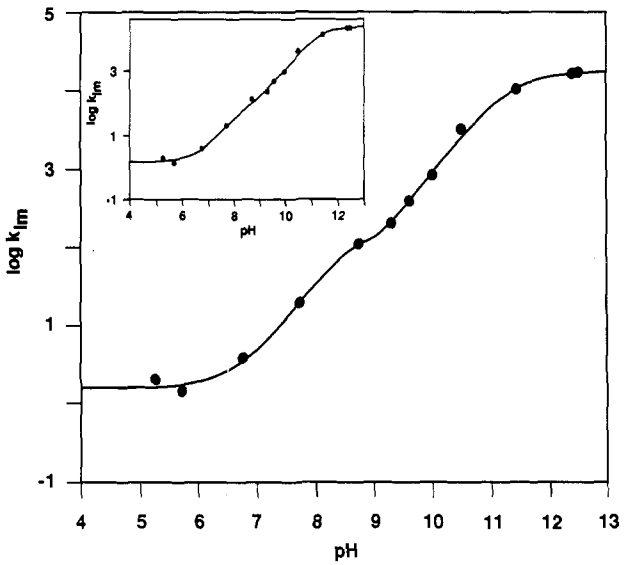

Figure 6. The pH dependence of the log of the nonbuffer-catalyzed rate constants (k_{Im}) for the reaction of (1)$Mn^{III}(X)_2$ with $(Ph)_2$(MeOCO)-COOH at saturating ImH concentrations. The points are experimentally determined rates for $ABTS^{\cdot+}$ formation (30 °C, μ = 0.2), and the curve was generated from eq 13. The inset represents the same points with a curve generated from eq 12.

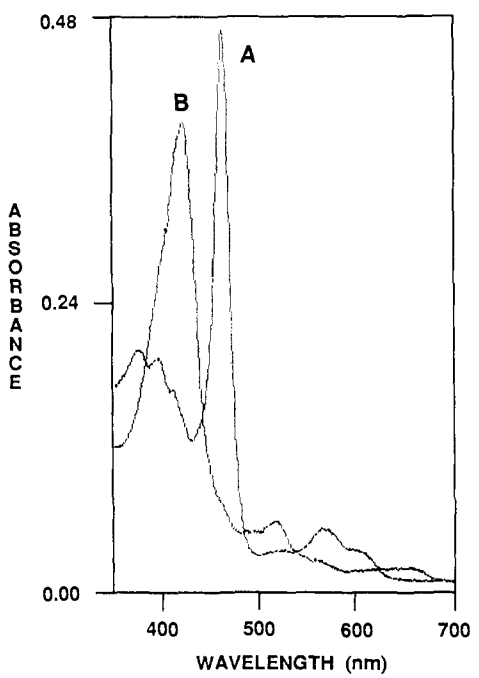

Figure 7. Visible absorption spectra of (1)$Mn^{III}(X)_2$ species in the absence and presence of ROOH ($[(1)Mn^{III}(X)_2]_i = 5.3 \times 10^{-6}$ M, $[(Ph)_2(MeOCO)COOH]_i = 6.62 \times 10^{-5}$ M, and [KOH] = 0.1 M (30 °C, μ = 0.2). Spectrum A is that of (1)$Mn^{III}(OH)_2$, while spectrum B corresponds to that of the manganese(IV) species formed after the addition of $(Ph)_2$(MeOCO)COOH.

the high-valent species to manganese(III). The absorption spectrum of the paramagnetic oxidized product of (1)$Mn^{III}(X)_2$ (Figure 7) showed an intense B band at 423 nm (ϵ = 76000) and two weak Q bands at 519 nm (ϵ = 12000) and 656 nm (ϵ = 4200) that is characteristic of a manganese(IV) porphyrin species.[14-18] The magnetic moment measured in aqueous solution (D_2O/DO^- buffer) by the Evans' technique[19] is 3.90 ± 0.10 μ_B at 295 K. This is consistent with an $S = {}^3/_2$ ground state for which the anticipated spin only value is 3.87 μ_B and is indicative of a high-spin, d^3, Mn(IV) complex. Reactions carried out in the presence of saturating concentrations of imidazole at pH 12.6 also showed the formation of high-valent manganese porphyrin species. The ab-

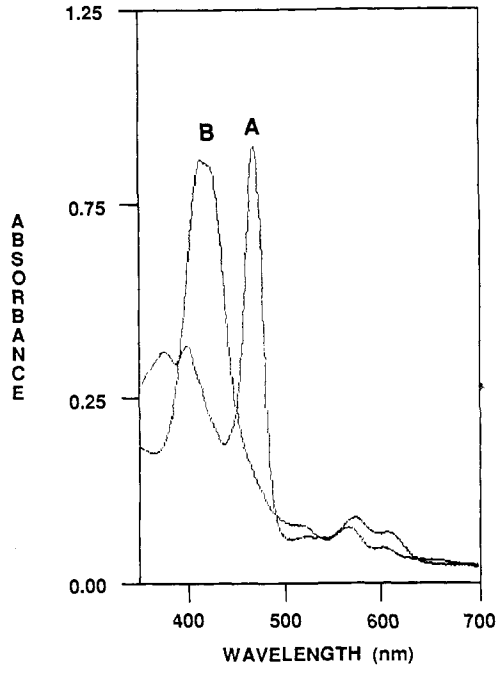

Figure 8. Visible absorption spectra of (1)$Mn^{III}(X)_2$ species at saturating concentrations of imidazole in the absence and presence of $(Ph)_2$(MeO-CO)COOH ([(1)$Mn^{III}(X)_2$]$_i$ = 5.3 × 10^{-6} M, [$(Ph)_2$(MeOCO)COOH]$_i$ = 6.62 × 10^{-5} M, [ImH]$_i$ = 1.0 × 10^{-2} M, and [KOH] = 0.1 M (30 °C, μ = 0.2). Spectrum A is that of [(1)Mn^{III}(OH)(Im)]$^-$ while spectrum B corresponds to that of the manganese(IV) species formed after the addition of $(Ph)_2$(MeOCO)COOH.

sorption spectrum (Figure 8) showed a broad B band centered at 419 nm (ϵ = 69000) and Q bands at 520 nm (ϵ = 5500), 566 nm (ϵ = 5300), and 603 nm (ϵ = 1600). We ascribe the high-energy shoulders present in the spectrum to overlapping peaks from the imidazolate-ligated and hydroxide-ligated manganese(IV) species.

Discussion

The reactions of the sterically blocked non-μ-oxo dimer-forming manganese(III) hydrates, (1)$Mn^{III}(X)_2$ and (2)$Mn^{III}(X)_2$ with $(Ph)_2$(MeOCO)COOH, have been investigated in water [pH 5.3–12.6, 30 °C with μ = 0.2 ($NaNO_3$)]. At all pH values examined, the reactions were first order in both [ROOH]$_i$ and [(porph)$Mn^{III}(X)_2$]$_i$, and the second-order rate constants (k_{ly}) were (i) independent of the concentration of the trapping agent ABTS; (ii) independent of the concentration of oxygen bases/oxygen acids and 2,4,6-trimethylpyridine or its conjugate acid (i.e., not subject to general base or general acid catalysis); and (iii) dependent on pH.

The dependence of the second-order rate constants (k_{ly}) on pH for the reactions of (1)$Mn^{III}(X)_2$ and (2)$Mn^{III}(X)_2$ with ROOH in aqueous solutions is shown in Figure 3. The data points in Figure 3 are experimental, and the lines were generated from the empirical eq 8 (based on Scheme I) with the derived constants reported in Table II. In Scheme I, the products arise from the decomposition of IV and V (eq 14). The sum of the concentrations

$$\frac{d[\text{Products}]}{dt} = -\frac{d[\text{ROOH}]}{dt} = k_2[\text{IV}] + k_3[\text{V}] \qquad (14)$$

of the porphyrin–manganese reactants I, II, and III is given by [Mn_t] = [I] + [II] + [III], and the sum of concentrations of intermediates is given by [I_t] = [IV] + [V]. The concentration of each intermediate species is expressed by eqs 15 and 16. Substituting the equalities of eqs 15 and 16 into eq 14 provides

$$[\text{IV}] = \frac{a_H}{K_{a3} + a_H}[I_t] \qquad (15)$$

$$[\text{V}] = \frac{K_{a3}}{K_{a3} + a_H}[I_t] \qquad (16)$$

Scheme I

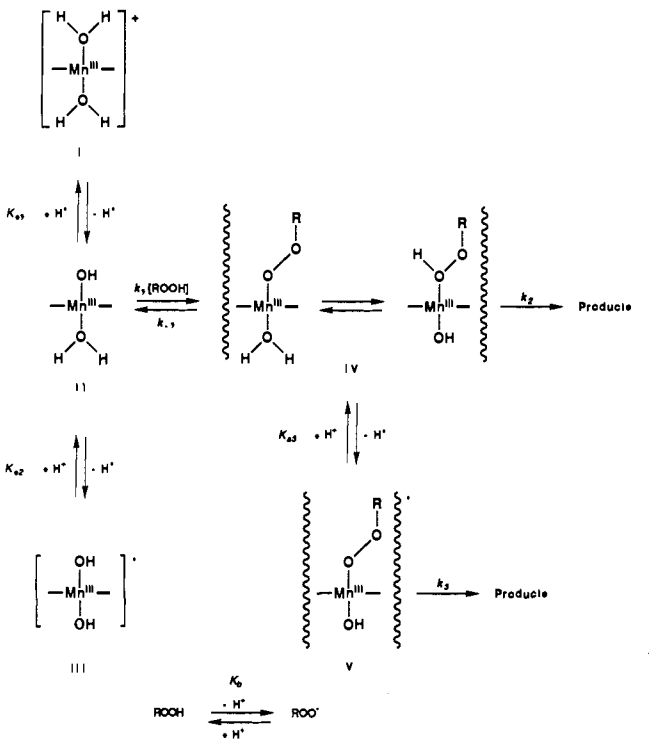

Scheme II

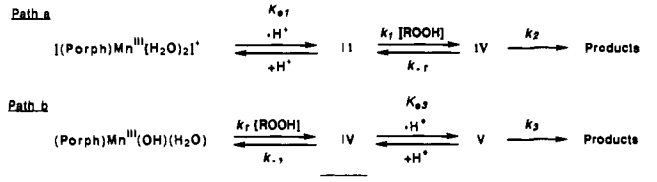

eq 17. Steady-state assumption in [I_t] and substitution of the value of [I_t] into eq 17 provides eq 18, where [$ROOH_t$] = [ROOH] + [ROO^-]. Rearrangement of eq 18 provides the full expression

$$\frac{d[\text{Products}]}{dt} = \frac{(k_2a_H + k_3K_{a3})(k_1K_{a1}a_H^2)[Mn_t][ROOH_t]}{\{(k_{-1} + k_2)a_H + k_3K_{a3}\}(a_H^2 + K_{a1}a_H + K_{a1}K_{a2})(K_b + a_H)} \qquad (18)$$

for the pH sensitive second-order rate constant k_{ly} (eq 19). Simplification of eq 19 gives eqs 20, 21, and 22. Equation 22 describes the sum of the terms contributing to k_{ly} in the different pH regions. The dependence of log k_{ly} on pH as shown in the pH profile of Figure 3 may be ascribed with paths a and b of Scheme II. The first term in eq 22 describes the lower plateau region of the pH profile which is given by path a of Scheme II. At higher pH values, the dependence of log k_{ly} on pH shows a "sigmoidal" shaped curve which is described by the second term in eq 22. This term refers to path b of Scheme II.

The values of the derived kinetic constants in Table II were obtained by computer fitting the experimental points of Figure 3 to eq 22. Although the values of the thermodynamic constants K_{a1} and K_{a2} have been previously determined[8c,20] (pK_{a1} = 5.8 and pK_{a2} = 12.2), the independent values of the other individual equilibrium constants and rate constants of Scheme I could not be determined without further assumptions since they appear as a collection of terms.

Comparison of the Second-Order Rate Constants for the Reactions of (1)$Mn^{III}(X)_2$ and (2)$Mn^{III}(X)_2$ with ROOH. From

$$k_{1y} = \frac{\left\{ \frac{k_1k_2}{(k_{-1}+k_2)} K_{a1} a_H^3 + \frac{k_1k_3}{(k_{-1}+k_2)} K_{a1}K_{a3}a_H^2 \right\}}{\left\{ \frac{k_3}{(k_{-1}+k_2)} K_{a3} + a_H \right\} (a_H^2 + K_{a1}a_H + K_{a1}K_{a2}) (K_b + a_H)} \quad (19)$$

$$k_{1y} = \frac{\left\{ \frac{k_1k_2}{(k_{-1}+k_2)} K_{a1} a_H^3 + \frac{k_1k_3}{(k_{-1}+k_2)} K_{a1}K_{a3}a_H^2 \right\}}{\left\{ a_H^3 + (K'' + K_{a1})a_H^2 + (K'' + K_{a2})K_{a1}a_H + K''K_{a1}K_{a2} \right\} (K_b + a_H)} \quad (20)$$

where $K'' = \frac{k_3}{(k_{-1}+k_2)} K_{a3}$, and neglecting a_H^3

$$k_{1y} = \frac{\left\{ \frac{k_1k_2}{(k_{-1}+k_2)} K_{a1} a_H^3 + \frac{k_1k_3}{(k_{-1}+k_2)} K_{a1}K_{a3}a_H^2 \right\} (K'' + K_{a1})^{-1}}{\left\{ \frac{K''K_{a1}K_{a2}}{(K'' + K_{a1})} + \frac{(K'' + K_{a2})}{(K'' + K_{a1})} K_{a1}a_H + a_H^2 \right\} (K_b + a_H)} \quad (21)$$

If $\frac{K''K_{a1}K_{a2}}{(K'' + K_{a1})} < \frac{(K'' + K_{a2})}{(K'' + K_{a1})} K_{a1}a_H$ at all pH values, and $a_H > K_b$

$$k_{1y} = \frac{k_1k_2K_{a1}}{\left\{k_3K_{a3} + (k_{-1}+k_2)K_{a1}\right\}} \left[\frac{a_H}{\frac{(K'' + K_{a2})}{(K'' + K_{a1})} K_{a1} + a_H} \right] + \frac{k_1k_3K_{a3}}{\left\{k_3K_{a3} + (k_{-1}+k_2)K_{a2}\right\}} \left[\frac{\frac{(K'' + K_{a2})}{(K'' + K_{a1})} K_{a1}}{\frac{(K'' + K_{a2})}{(K'' + K_{a1})} K_{a1} + a_H} \right] \quad (22)$$

Figure 3 it is seen that the rate constants for (**2**)$Mn^{III}(X)_2$ are greater than those for (**1**)$Mn^{III}(X)_2$ in the pH range 5.3–9.0. However, above pH 9.0 the rate constants for (**1**)$Mn^{III}(X)_2$ are greater than those for (**2**)$Mn^{III}(X)_2$. In any event, the maximum difference in rates obtained with the two manganese–porphyrins is, at most, only 10-fold. Hence, the replacement of the eight ortho-methyl substituents in (**1**)$Mn^{III}(X)_2$ by chloro substituents in (**2**)$Mn^{III}(X)_2$ does not greatly alter the reactivity toward ROOH in water. Since the orientation of the phenyl groups in (**1**)-$Mn^{III}(X)_2$ and (**2**)$Mn^{III}(X)_2$ are assumed to be perpendicular to the porphyrin plane, the π-interactions between the two systems are very limited.[21] Thus, changes in substituents on the phenyl group would not be expected to exert much influence on the electronic nature of the manganese center. Even smaller differences have been observed for the pH-dependent second-order rate constants for reaction of $(Ph)_2(MeOCO)COOH$ and *t*-BuOOH with (**1**)$Fe^{III}(X)_2$ and (**2**)$Fe^{III}(X)_2$.[8j-l]

Scheme III

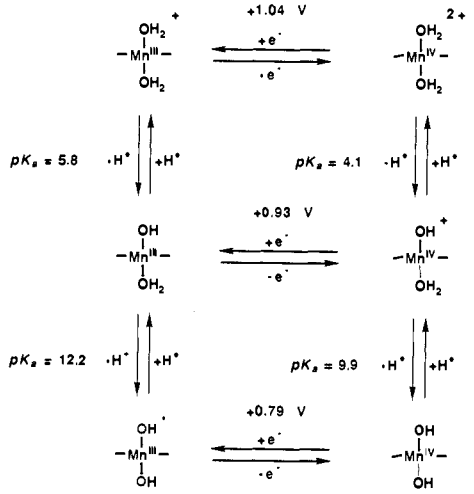

Mechanisms of Reactions. The independence from buffer and trapping agent (ABTS) concentrations plus the first-order dependence upon the concentrations of (porph)$Mn^{III}(X)_2$ and $(Ph)_2(MeOCO)COOH$, shows that the transition states of the rate-determining steps, at all pH values, comprise only of (porph)$Mn^{III}(X)_2$ with $(Ph)_2(MeOCO)COOH/(Ph)_2(MeOCO)COO^-$. The products of the reactions were determined to be benzophenone and $(Ph)_2(MeOCO)COH$. The formation of benzophenone may be explained by the fragmentation of $(Ph)_2(MeOCO)CO^\bullet$ formed as a result of (porph)$Mn^{III}(X)_2$-catalyzed homolytic O–O bond cleavage (eqs 23 and 24). The formation

$$(\mathbf{1})Mn^{III}(X)((Ph)_2(MeOCO)COOH) \rightarrow \{(\mathbf{1})Mn^{IV}(X)_2 + (Ph)_2(MeOCO)CO^\bullet\} \quad (23)$$

$$\{(\mathbf{1})Mn^{IV}(X)_2 + (Ph)_2(MeOCO)CO^\bullet\} \rightarrow (\mathbf{1})Mn^{IV}(X)_2 + (Ph)_2CO + CO_2 + Me^\bullet \quad (24)$$

$$\{(\mathbf{1})Mn^{IV}(X)_2 + (Ph)_2(MeOCO)CO^\bullet\} \rightarrow (\mathbf{1})Mn^{V}(O)(X) + (Ph)_2(MeOCO)COH \quad (25)$$

of $(Ph)_2(MeOCO)COH$ may be explained by either homolytic cleavage of the O–O bond followed by H• transfer (eqs 23 and 25) or by manganese–porphyrin-catalyzed heterolytic cleavage of the O–O bond (eq 26).

$$(\mathbf{1})Mn^{III}(X)((Ph)_2(MeOCO)COOH) \rightarrow (\mathbf{1})Mn^{V}(O)(X) + (Ph)_2(MeOCO)COH \quad (26)$$

Observations on the Formation of a Manganese(IV) Porphyrin Intermediate. In the absence of ABTS the buildup of a manganese(IV) porphyrin species is observed. Although the observed formation of a (porph)$Mn^{IV}(X)_2$ species may be in accord with a homolytic reaction, its appearance is not uniquely explained by such a mechanism since a manganese(V) species will rapidly undergo comproportionation with manganese(III) to provide a manganese(IV) species. The transformation of manganese(III) porphyrin to manganese(IV) porphyrin is incomplete at pH 8.9, but the manganese(IV) porphyrin is formed in 100% yield at pH 12.6, where it is stable for periods of several hours. This observation on the stability of the manganese(IV) species at higher pH's is supported by the finding that high-valent manganese species are stabilized by hydroxide ligation.[18] It has been shown from electrochemical studies that the exchange of a Cl^- for HO^- as the axial ligand changes the product of the oxidation from a porphyrin-centered manganese(III) porphyrin π-cation radical to a metal-centered manganese(IV) porphyrin. Thus change of axial ligation from H_2O to HO^- at higher pH values must contribute significantly to the stability of the manganese(IV) species.

The question arises as to what is the nature of the axial ligand in water. Recent electrochemical studies from this laboratory[20] have established the structures, acid dissociation constants, and

(14) Camenzind, M. J.; Hollander, F. J.; Hill, C. L. *Inorg. Chem.* **1982**, *21*, 4301.
(15) (a) Bortolini, O.; Meunier, B. *J. Chem. Soc., Chem. Commun.* **1983**, 1364. (b) Bortolini, O.; Ricci, M.; Meunier, B.; Priant, P.; Ascone, I.; Goulon, J. *Nouv. J. Chim.* **1986**, *10*, 39.
(16) Spreer. L. O.; Maliyackel, A. C.; Holbrook, S.; Otvos, J. W.; Calvin, M. *J. Am. Chem. Soc.* **1986**, *108*, 1949.
(17) (a) Groves, J. T.; Stern, M. K. *J. Am. Chem. Soc.* **1987**, *109*, 3812. (b) Groves, J. T.; Stern, M. K. *J. Am. Chem. Soc.* **1988**, *110*, 8628.
(18) Arasasingham, R. D.; Bruice, T. C. *Inorg. Chem.* **1990**, *29*, 1442.
(19) Evans, D. F. *J. Am. Chem. Soc.* **1959**, *81*, 2003.
(20) Kaaret, T. W.; Zhang, G.-H.; Bruice, T. C. *J. Am. Chem. Soc.* **1991**, *113*, 4652.
(21) (a) Walker, F. A.; Balke, V. L.; Mcdermott, G. A. *Inorg. Chem.* **1982**, *21*, 3342. (b) Walker, F. A.; Buehler, J.; West, J. T.; Hinds, J. L. *J. Am. Chem. Soc.* **1983**, *105*, 6923. (c) Mcdermott, G. A.; Walker, F. A. *Inorg. Chim. Acta* **1984**, *91*, 95.

Scheme IV

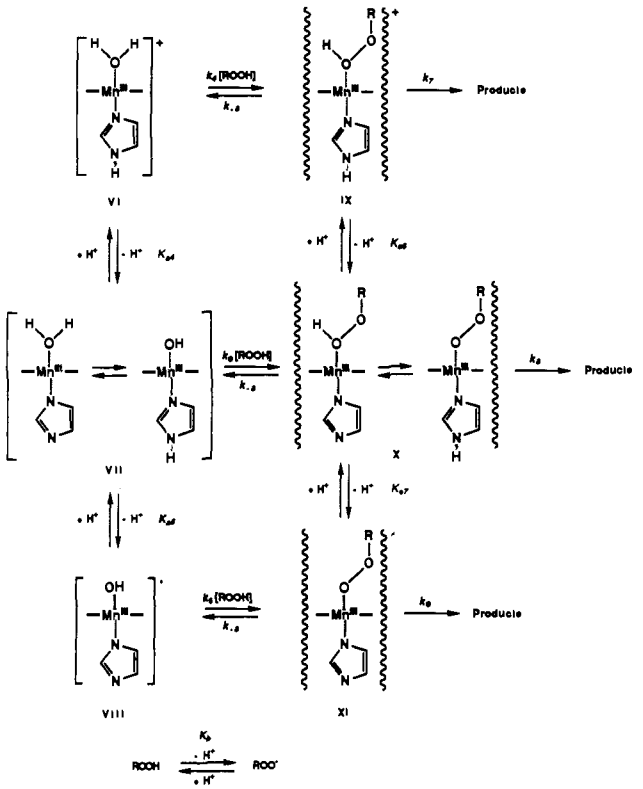

potentials for the one-electron oxidation of (1)$Mn^{III}(X)_2$ in water as a function of pH (Scheme III). Inspection of Scheme III shows that in water only H_2O and HO^- serve as axial ligands to the $[(porph)Mn^{IV}]^{2+}$ species. At pH values above ~12, the structures $(porph)Mn^{IV}(OH)_2$ and $(porph)Mn^{IV}(=O)(H_2O)$ are equivalent. In the case of reactions with ROOH, at pH values above ~12, the immediate product of an oxygen-transfer reaction involving a homolytic scission of the O–O bond would be $[(porph)Mn^{IV}(=O)(OH)]^-$.

Effect of Imidazole Ligation on the Reaction of (1)$Mn^{III}(X)_2$ with ROOH. Spectrophotometric titrations have established that (1)$Mn^{III}(X)_2$ ligates to only one imidazole. The value for the equilibrium constant for monoligation of imidazole obtained by kinetic means ($\log K_1 = 2.43 \pm 0.05$, $\mu = 0.2$) compares well with the value ($\log K_1 = 2.20 + 0.05$, $\mu = 1.0$) determined by spectrophotometric titration.[8c] The slight difference in the determined values of K_1 is attributed to the different ionic strengths employed in the two determinations (see Results).

At saturating concentrations of imidazole (ImH), the manganese porphyrin is present as the monoligated species, (1)Mn^{III}(ImH)(X). The reaction of (1)Mn^{III}(ImH)(X) with $(Ph)_2(MeOCO)COOH$ is kinetically first-order in both components. The pH dependence of the apparent second-order rate constants (k_{1m}) is provided in Figure 6. The experimental points in Figure 6 were fit to the empirical eq 13 with the derived constants reported in Table III. The proposed series of reactions which account for the pH dependence of k_{1m} are shown in Scheme IV.

In the derivation of eq 13 the assumption was made that the intermediates IX, X, and XI are at steady state. The mathematical form of the kinetic expression remains the same regardless of whether K_{a6} and K_{a7} are included or not. The simplest expression is obtained when K_{a6} and K_{a7} are ignored. The products of the reactions arise from the decomposition of intermediates IX, X, and XI (eq 27). Assuming steady-state in [IX], [X], and [XI]

$$\frac{d[\text{Products}]}{dt} = \frac{d[\text{ROOH}]}{dt} = k_7[\text{IX}] + k_8[\text{X}] + k_9[\text{XI}] \qquad (27)$$

the concentration of each intermediate species is expressed in eqs 28, 29, and 30, where $[Mn_t] = [VI] + [VII] + [VIII]$ and

Scheme V

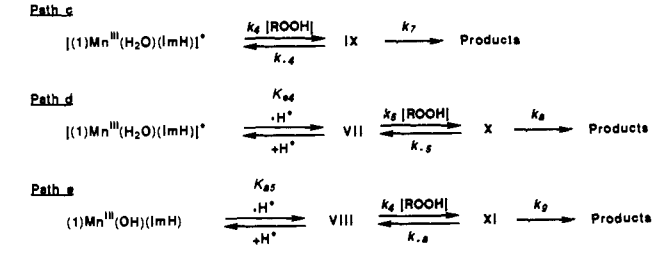

$[ROOH_t] = [ROOH] + [ROO^-]$. Substituting the equalities of eqs 28, 29, and 30 into eq 27 provides eq 31. Rearrangement of

$$[\text{IX}] = \frac{k_4}{(k_{-4} + k_7)} \frac{a_H^3}{(a_H^2 + K_{a4}a_H + K_{a4}K_{a5})(K_b + a_H)} [Mn_t][ROOH_t] \qquad (28)$$

$$[\text{X}] = \frac{k_5}{(k_{-5} + k_8)} \frac{K_{a4}a_H^2}{(a_H^2 + K_{a4}a_H + K_{a4}K_{a5})(K_b + a_H)} [Mn_t][ROOH_t] \qquad (29)$$

$$[\text{XI}] = \frac{k_6}{(k_{-6} + k_9)} \frac{K_{a4}K_{a5}a_H}{(a_H^2 + K_{a4}a_H + K_{a4}K_{a5})(K_b + a_H)} [Mn_t][ROOH_t] \qquad (30)$$

eq 31 to provide eq 32 yields the full expression for the pH sensitive

$$\frac{d[\text{Products}]}{dt} = \frac{\left\{\frac{k_4k_7}{(k_{-4} + k_7)} a_H^3 + \frac{k_5k_8}{(k_{-5} + k_8)} K_{a4}a_H^2 + \frac{k_6k_9}{(k_{-6} + k_9)} K_{a4}K_{a5}a_H\right\}[Mn_t][ROOH_t]}{(a_H^2 + K_{a4}a_H + K_{a4}K_{a5})(K_b + a_H)} \qquad (31)$$

second-order rate constants k_{1m}. Computer fitting of the experimental points to eq 32 provides a set of constants whose relative values allow simplification of eq 32 in the different pH regions.

$$k_{1m} = \frac{\left\{\frac{k_4k_7}{(k_{-4} + k_7)} a_H^3 + \frac{k_5k_8}{(k_{-5} + k_8)} K_{a4}a_H^2 + \frac{k_6k_9}{(k_{-6} + k_9)} K_{a4}K_{a5}a_H\right\}}{(a_H^2 + K_{a4}a_H + K_{a4}K_{a5})(K_b + a_H)} \qquad (32)$$

At pH values below 5.5, $a_H > K_{a4}$, K_{a5}, K_b such that eq 32 reduces to eq 33. Thus, this describes the lower plateau region of the pH profile, and the reaction is given by path c of Scheme V.

$$k_{1m} = \frac{k_4k_7}{(k_{-4} + k_7)} \frac{a_H}{(K_{a4} + a_H)} \qquad (33)$$

Between pH 5.5 and 9.5, the dependence of $\log k_{1m}$ describes a "bell-shaped" curve. Here $k_{a5} < a_H > K_b$ so that eq 32 reduces to eq 34, which pertains to path d of Scheme V. The rate increase in the ascending part of the bell results from the increased ionization of VI to VII with increase in pH until all of $[(1)Mn^{III}(H_2O)(ImH)]^+$ is depleted, whereupon the ligation of ROOH with (1)Mn^{III}(OH)(ImH) becomes rate-limiting. This results in a drop in the rate. This portion of the profile overlaps with that of the term shown in eq 35.

$$k_{1m} = \frac{k_5k_8}{(k_{-5} + k_8)} \frac{K_{a4}a_H}{(a_H^2 + K_{a4}a_H + K_{a4}K_{a5})} \qquad (34)$$

Above pH 10, $\log k_{1m}$ increases with pH with a slope of one, and above pH ~11 $\log k_{1m}$ becomes pH independent. In this pH range $K_b < a_H > K_{a4}$, K_{a5} and $K_{a4}a_H > a_H^2$ so that eq 32 simplifies to eq 35 (path e, Scheme V). In this pH range the plot is that expected for the ionization of a monoprotic acid $[(1)Mn^{III}(ImH)(OH) \rightarrow (1)Mn^{III}(Im)(OH) + H^+; K_{a5})$.

$$k_{1m} = \frac{k_6k_9}{(k_{-6} + k_9)} \frac{K_{a5}}{(K_{a5} + a_H)} \qquad (35)$$

Summation of the terms contributing to k_{1m} in the different pH regions provides eq 36. This describes the dependence of k_{1m}

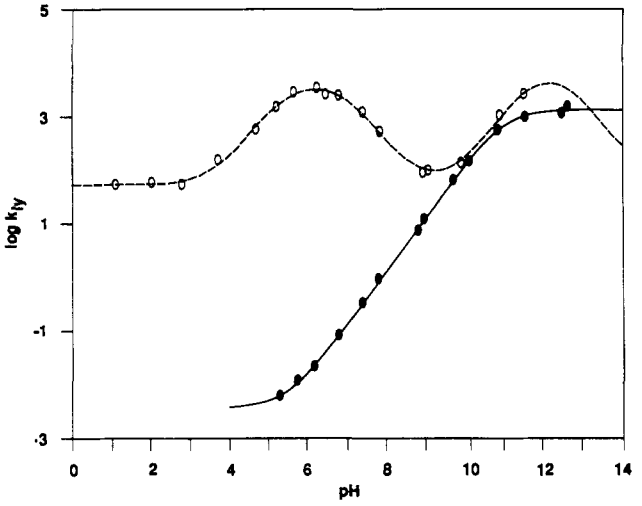

Figure 9. Comparison of the plots of log k_{ly} vs pH for the reactions of $(Ph)_2(MeOCO)COOH$ with $(1)Mn^{III}(X)_2$ (solid line, this study) and $(1)Fe^{III}(X)_2$ (dashed line, preceding paper in this issue). The two sets of points are experimental while the lines were generated by computer fitting the appropriate rate equations (see Discussion).

on pH over the entire pH range using paths c, d, and e of Scheme V.

$$k_{lm} = \frac{k_4k_7}{(k_{-4}+k_7)}\frac{a_H}{(K_{a4}+a_H)} + \frac{k_5k_8}{(k_{-5}+k_8)}\frac{K_{a4}a_H}{(a_H^2+K_{a4}a_H+K_{a4}K_{a5})} + \frac{k_6k_9}{(k_{-6}+k_9)}\frac{K_{a5}}{(K_{a5}+a_H)} \quad (36)$$

A comparison of the pH dependence of the second-order rate constants k_{ly} and k_{lm} for the reaction of $(1)Mn^{III}(X)_2$ (Figure 3) and $(1)Mn^{III}(X)(ImH)$ (Figure 6), respectively, shows that imidazole ligation provides about a ~100-fold rate enhancement. That the rate enhancement is due to ligation of imidazole is supported by the studies with nonligating 2,4,6-trimethylpyridine. Addition of 2,4,6-trimethylpyridine was found to have no influence on the rate of reaction of ROOH with $(1)Mn^{III}(X)_2$. The displacement of H_2O or HO^- axial ligands by imidazole in protic solvents occurs due to the more favorable electron donor properties of nitrogenous ligands. According to our proposal of mechanism (Scheme IV), the species present at high pH is an imidazolate anion ligated manganese(III) porphyrin. The kinetically determined acid dissociation constant of eq 37 (pK_{a5} = 11.3) may be compared to that of ImH in water (pK_a = 14.6).[22] The counterpart

$$(1)Mn^{III}(OH)(ImH) \rightleftharpoons [(1)Mn^{III}(OH)(Im)]^- + H^+ \quad (37)$$

to the spontaneous decomposition of the complex $(1)Mn^{III}(OOR)(Im) \rightarrow (1)Mn^{IV}(O)(Im) + RO^\bullet$ in water is the established catalysis by proximal hydrogen bonding of free ImH to the ligated ImH in the oxygen-transfer reactions from *t*-BuOOH to *meso*-tetraphenylporphinatomanganese(III) chloride in aprotic solvent.[23]

A Comparison of the pH Dependence for the Reaction of Manganese(III) and Iron(III) Porphyrins with Hydroperoxides. The log k_{ly} vs pH profiles for the reaction of $(1)Mn^{III}(X)_2$ and $(1)Fe^{III}(X)_2$ with $(Ph)_2(MeOCO)COOH$ are provided in Figure 9. The shape of the profiles for reaction of $(1)Fe^{III}(X)_2$ with $(Ph)_2(MeOCO)COOH$ is typical of that seen with (porph)-$Fe^{III}(X)_2$ and alkyl hydroperoxides [i.e., $(1)Fe^{III}(X)_2$ with *t*-BuOOH and $Ph(Me)_2COOH$ and $(2)Fe^{III}(X)_2$ with *t*-BuOOH]. The first aspect to be noticed is that though the second-order rate constants for reaction of $(1)Mn^{III}(X)_2$ and $(1)Fe^{III}(X)_2$ are comparable at high pH, the $(1)Fe^{III}(X)_2$ species is much more reactive at low pH. Secondly, the shape of the profiles are very different for manganese(III) and iron(III) porphyrins.

Both lines of Figure 9 have been generated from equations which assume steady state in metal porphyrin species ligated to hydroperoxide species. The reaction schemes for $(1)Mn^{III}(X)_2$ (Scheme I of this study) and $(1)Fe^{III}(X)_2$ (Scheme I of the preceding paper in this issue) are identical with the exception that in the case of the iron(III) porphyrin all hydroperoxide-ligated species present in solution undergo oxidative oxygen transfer (i.e., $[(1)Fe^{III}(H_2O)(ROOH)]^+$, $(1)Fe^{III}(OH)(ROOH)/(1)Fe^{III}(H_2O)(ROO)$, and $[(1)Fe^{III}(OH)(ROO)]^-$, while in the case of $(1)Mn^{III}(X)_2$ the reactive species are $(1)Mn^{III}(OH)(ROOH)/(1)Mn^{III}(H_2O)(ROO)$ and $[(1)Mn^{III}(OH)(ROO)]^-$. Similar differences are observed in the reaction of hydrogen peroxide with $(1)Fe^{III}(X)_2$ [or $(2)Fe^{III}(X)_2$] and $(1)Mn^{III}(X)_2$.[8c]

A comparison of the potentials for the $1e^-$ oxidation[20] of $[(1)Mn^{III}(H_2O)_2]^+$ (low pH), $(1)Mn^{III}(OH)(H_2O)$ (intermediate pH), and $[(1)Mn^{III}(OH)_2]^-$ (high pH) with $[(1)Fe^{III}(H_2O)_2]^+$, $(1)Fe^{III}(OH)(H_2O)$, and $[(1)Fe^{III}(OH)_2]^-$ shows that the change in potential from iron to manganese for the different species is 130, 70, and 20 mV, respectively. This is equivalent to a change in free energy of activation ($\Delta\Delta G^\ddagger$) of ~3.0, 1.6, and 0.5 kcal·mol^{-1}, respectively. Thus, for the different species, the $\Delta\Delta G^\ddagger$ values would predict a $k_{ly}^{(1)Fe(X)_2}/k_{ly}^{(1)Mn(X)_2}$ ratio of ~158, 15, and 2, respectively. Consistent with this observation, examination of Figure 9 shows that at higher pH, the second-order rate constants of $(1)Mn^{III}(X)_2$ and $(1)Fe^{III}(X)_2$ are comparable, while at lower pH the $(1)Fe^{III}(X)_2$ is far more reactive.

Acknowledgment. This work was supported by a grant from the National Institutes of Health.

(22) Bruice, T. C.; Herz, J. L. *J. Am. Chem. Soc.* **1964**, *86*, 4109.
(23) Yuan, L.-C.; Bruice, T. C. *J. Am. Chem. Soc.* **1986**, *108*, 1643.